A Base-Catalyzed Mechanism for Dark State Recovery in the *Avena sativa* Phototropin-1 LOV2 Domain†

Maxime T. A. Alexandre,*,‡ Jos C. Arents,§ Rienk van Grondelle,‡ Klaas J. Hellingwerf,§ and John T. M. Kennis‡

Department of Biophysics, Faculty of Sciences, Vrije Universiteit, De Boelelaan 1081, 1081HV Amsterdam, The Netherlands, and Swammerdam Institute for Life Sciences, University of Amsterdam, Amsterdam, The Netherlands

Received October 5, 2006; Revised Manuscript Received December 18, 2006

ABSTRACT: Phototropins are autophosphorylating serine/threonine kinases responsible for blue-light perception in plants; their action gives rise to phototropism, chloroplast relocation, and opening of stomatal guard cells. The kinase domain constitutes the C-terminal part of *Avena sativa* phototropin 1. The N-terminal part contains two light, oxygen, or voltage (LOV) sensing domains, LOV1 and LOV2; each binds a flavin mononucleotide (FMN) chromophore ($\lambda^{max} = 447$ nm, termed D_{447}) and forms the light-sensitive domains, of which LOV2 is the principal component. Blue-light absorption produces a covalent adduct between a very conserved nearby cysteine residue and the C(4a) atom of the FMN moiety via the triplet state of the flavin. The covalent adduct thermally decays to regenerate the D_{447} dark state, with a rate that may vary by several orders of magnitude between different species. We report that the imidazole base can act as a very efficient enhancer of the dark recovery of *A. sativa* phot1 LOV2 (AsLOV2) and some other well-characterized LOV domains. Imidazole accelerates the thermal decay of AsLOV2 by 3 orders of magnitude in the submolar concentration range, via a base-catalyzed mechanism involving base abstraction of the FMN N(5)−H adduct state and subsequent reprotonation of the reactive cysteine. The LOV2 crystal structure suggests that the imidazole molecules may act from a cavity located in the vicinity of the FMN, explaining its high efficiency, populated through a channel connecting the cavity to the protein surface. Use of pH titration and chemical inactivation by diethyl pyrocarbonate (DEPC) suggests that histidines located at the surface of the LOV domain act as base catalysts via an as yet unidentified H-bond network, operating at a rate of $(55\ s)^{-1}$ at pH 8. In addition, molecular processes other than histidine-mediated base catalysis contibute significantly to the total thermal decay rate of the adduct and operate at a rate constant of $(65\ s)^{-1}$, leading to a net adduct decay time constant of 30 s at pH 8.

Phototropins are responsible for blue-light perception in plants which leads to phototropism, chloroplast relocation, and opening of stomatal guard cells (*1*). The phototropins are serine/threonine kinases that undergo autophosphorylation in response to absorption of blue light (*2*). Several phototropin homologues were discovered in plants, algae, fungi, and bacteria, and it was proposed that they act as photoreceptors in their respective organisms (*3*−*7*). Two light, oxygen, or voltage (LOV) sensing domains, LOV1 and LOV2, each bind a flavin mononucleotide (FMN) chromophore and form the light-sensitive domains of phototropins, of which LOV2 is the principal component. In the dark-adapted state of LOV2, also termed D_{447} after its absorption maximum (*8*), FMN is noncovalently bound to the protein via a number of hydrogen bonds and nonpolar and polar interactions (*9*, *10*). Blue-light absorption promotes the noncovalently bound FMN to its singlet excited state, which in turn evolves to the triplet state with a high efficiency (*8*, *11*, *12*). From the triplet state, a covalent adduct between a very conserved nearby cysteine residue and the C4a atom of the FMN moiety is formed. This state is termed S_{390} (*8*−*10*, *13*−*16*) and is thought to correspond to the signaling state of the LOV domain that promotes kinase activation (*1*). The covalent adduct thermally decays to regenerate the D_{447} dark state at a rate that may vary by several orders of magnitude between LOV domains from different species (*17*), as shown in Figure 1a. Absorption of near-UV light by the S_{390} state also leads to rupture of the covalent adduct (*12*, *18*). For convenience, the D_{447} and S_{390} states will be called the dark and light state, respectively.

The dark recovery rates of the covalent adduct (S_{390}) vary widely among the various LOV domains, from seconds to minutes in isolated phototropin LOV1 and LOV2 domains (*12*, *15*, *17*, *19*) to hours in some bacterial LOV proteins (*3*, *20*). In the LOV domains involved in circadian regulation in *Arabidopsis*, the covalent adduct does not decay at all (*6*). These observations indicate that in the phot LOV domains with a fast recovery rate (up to 1 s^{-1}) the disruption of the covalent adduct must be facilitated.

On the basis of the observed pH dependence, the dark recovery was proposed to be base-catalyzed in *Avena sativa*

† M.T.A.A. was supported by the Life Sciences Councel of the Netherlands Organization for Scientific Research (NWO-ALW) through the 'Molecule to Cell' programme. J.T.M.K. was supported by NWO-ALW through a VIDI fellowship.

* To whom correspondence should be addressed. E-mail: miaalex@nat.vu.nl. Phone: +31-(0)20-59 87932. Fax: +31-(0)20-5987999.

‡ Vrije Universiteit.

§ University of Amsterdam.

10.1021/bi062074e CCC: $37.00
Published on Web 02/21/2007

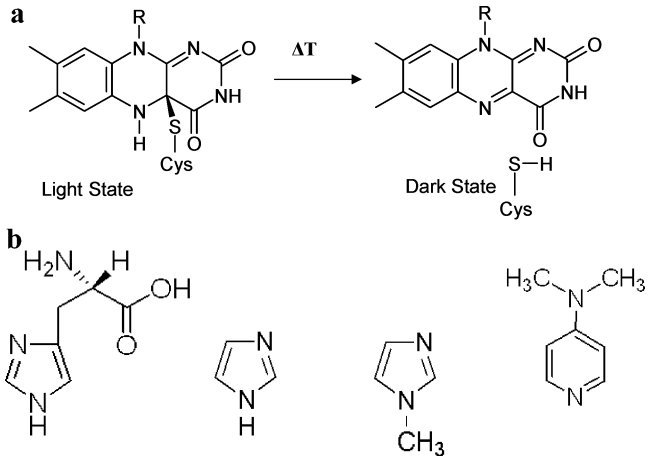

FIGURE 1: (a) Schematic structure of the chromophore binding pocket of the LOV domain in the signaling state of receptor state thermal decay. (b) Schematic structures of L-histidine, imidazole, 1-methylimidazole, and dimethylaminopyridine from left to right. All molecules are shown in the basic form.

(oat) phot1 LOV2 (AsLOV2)[1] (*8*), *Chlamydomonas reinhardtii* phot LOV1 (CrLOV1) (*12*), and *C. reinhardtii* phot LOV2 (CrLOV2) (*19*). According to the *Adiantum* phy3 LOV2 and CrLOV1 crystal structures, no basic amino acids are located in the vicinity of the FMN (*9*, *10*). Swartz et al. suggested that two histidines 14 and 12 Å from the FMN, respectively, on the AsLOV2 surface are possible candidates, from which base-facilitated catalysis may proceed, via a hydrogen bonding network among the base, chromophore, and intraproteineous water molecules (*8*). For CrLOV1 and CrLOV2, the dark recovery rate was shown to depend on the salt concentration. To explain the salt dependence, Kottke and Guo proposed the involvement of the FMN phosphate in the regulation of the dark recovery rate (*12*, *19*). The adduct decay rate slows significantly in LOV1−LOV2 tandem constructs and in the full-length phot1 receptor (*17*, *19*), indicating that protein−protein interactions are important for the rate of recovery as well. Finally, the dark recovery was shown to be thermally activated, and energetic barriers defined by the extent of conformational change of the LOV domain very likely also partly define the rate of adduct decay (*12*, *19*, *21*−*23*).

The work presented here shows that the imidazole base can act as a very efficient enhancer of the rate of dark recovery of AsLOV2 and several other well-characterized LOV domains. Imidazole accelerates the thermal decay of D_{447} of AsLOV2 by 3 orders of magnitude in the submolar concentration range, via a base-catalyzed mechanism, involving base abstraction of the adduct state from FMN N(5)−H and subsequent reprotonation of the reactive cysteine. Moreover, using pH titration and diethyl pyrocarbonate (DEPC) inactivation, we demonstrate that histidines located at the surface of the LOV domain act as a natural base catalysts via an as yet unidentified H-bond network. This imidazole effect opens a new avenue for the application of spectroscopy to LOV domains which need relatively high repetition rates, such as step-scan FTIR.

[1] Abbreviations: phot, phototropin; AsLOV2, *Avena sativa* phot1 LOV2; CrLOV1, *Chlamydomonas reinhardtii* phot LOV1; CrLOV2, *C. reinhardtii* phot LOV2; phy3LOV2, *Adiantum capillus-veneris* phy3LOV2; DEPC, diethyl pyrocarbonate; DMAP, dimethylaminopyridine.

MATERIALS AND METHODS

Expression and Purification of LOV2. The LOV2 domain from *A. sativa* (oat) phototropin 1 was expressed and purified as previously described (*24*). *A. sativa* phototropin 1 LOV2 was expressed from a construct spanning residues 404−560 (construct generously provided by K. Gardner of the University of Texas Southwestern Medical Center, Dallas, TX). Because in this work the effect of imidazole on AsLOV2 has been studied, it is particularly important to ensure complete removal of imidazole. To do so, the collected fractions containing AsLOV2 from the His-Trap HP column (GE Healthcare) were further purified using a 6 mL Resource Q ion-exchange column (GE Healthcare) using a NaCl gradient and dialyzed against a buffer containing 20 mM Tris-HCl (pH 8) and 50 mM NaCl (10 mL of AsLOV2 against 5 L of buffer). The sample was stored in 20 mM Tris-HCl (pH 8) and 50 mM NaCl. The MBP−CrLOV2 sample was kindly donated by P. Hegemann of Humboldt University (Berlin, Germany).

Imidazole and imidazole analogues, 1-methylimidazole, dimethylaminopyridine (DMAP), and histidine were obtained from Sigma Chemicals Ltd., as were azide, GnCl, and DEPC.

Transient (milliseconds to seconds) UV−Vis Measurements. Slow (subseconds to hours) UV−vis transient absorption spectra were recorded with a model 8453 Hewlett-Packard diode array spectrophotometer (Portland, OR), which has a time resolution of 0.1 s. Typically, UV−vis difference spectra were recorded from 280 to 550 nm. A Schott KL1500 light source (containing a 150 W halogen lamp) connected to a glass fiber in combination with a heat filter and a 100 nm band-pass filter with maximum transmission at 450 nm was used for continuous illumination. The fluence rate of the actinic light was approximately 3000 μmol m^{-2} s^{-1}.

Laser-Flash Photolysis Spectroscopy. For fast visible transient absorption measurements, an Edinburgh Instruments Ltd. LP900 spectrometer (Livingston, West Lothian, U.K.) was used, equipped with a photomultiplier slow board detection system connected to an oscilloscope (Tektronix TDS 340A) in combination with a Continuum Surelite I-10 Nd:YAG laser (output intensity of 140 mJ at 355 nm; pulse width of 6 ns). The AsLOV2 sample was excited with 355 nm laser flashes of 2−3 mJ/pulse at a frequency of 0.5 Hz. Time traces were recorded at 450 nm with the slow board option of the photomultiplier (time resolution of 2 ms). For each measurement, 50 traces have been averaged to increase the signal-to-noise ratio. Optical neutral density filters were used in the measuring beam before the sample to minimize measurement artifacts induced by probe light.

Data Analysis. For the initial analysis, the fitting tools of Origin 6.0 (Microcal Software, Inc.) were used. Time traces at 475 and 450 nm were satisfactorily fitted with a single-exponential function for both the slow and fast measurements.

Effect of Imidazole on AsLOV2 Dark Recovery. Enhancement of the dark recovery rate by imidazole was analyzed using AsLOV2 samples in 20 mM Tris-HCl and 50 mM NaCl (pH 8). For the transient UV−vis experiments, the sample was incubated with imidazole concentrations ranging

from 0.4 to 100 mM and from 150 to 660 mM for the slow and fast time-resolved experiments, respectively. All added solutions were set at pH 8 using HCl or NaOH. No free FMN was found in the flow-through after concentration (Centicon YM 10, Amicon, Beverly, MA) and dilution of the sample three times in the presence of 1 M imidazole, showing that the amplitude changes are not induced by either inactivation of AsLOV2 by imidazole or release of FMN.

Identification of the Active Form of Imidazole. To determine which form of imidazole, i.e., the acidic or basic form, is responsible for the enhancement of the dark recovery rate, the pH dependence of the effect of imidazole on AsLOV2 was analyzed in 20 mM Tris-HCl and 50 mM NaCl at pH 8 and 20 mM MOPS-HCl and 50 mM NaCl at pH 7. The D_{447} state recovery was measured with the Hewlett-Packard 8453 spectrophotometer using imidazole concentrations between 0.4 and 100 mM, after adding small volumes from a 2 M imidazole stock solution adjusted to pH 8 and pH 7, respectively.

pH Titration of the Rate of Dark Recovery of AsLOV2. The pH titration of ground state recovery of AsLOV2 in 100 mM KP_i and 50 mM NaCl was started at pH 6.4. Below this pH, the protein starts to precipitate. The pH was increased in a stepwise manner to 11.5 using 1 M NaOH. Absorption and pH signals were measured simultaneously at 293 K by placing a Peltier temperature-controlled "Kraayenhof vessel" in the sample compartment of the Hewlett-Packard 8453 spectrophotometer. Two of the four available ports of the vessel were used for the measurement beam of the spectrophotometer, and a third was used for a pH electrode (Mettler Toledo micro-AgCl combination electrode, InLab 423) connected to a Dulas Engineering amplifier (pH-meter, input impedance of 10^{13} Ω). Continuous actinic illumination was provided through the fourth port of the vessel by a Schott KL1500 light source, equipped with a glass fiber in combination with a heat filter and a 450 nm band-pass filter. AsLOV2 was used at an OD of 0.5 at 447 nm in a working volume of 1.8−2 mL. The electrode was calibrated with calibration buffers of pH 4.01, 6.98, and 9.18 (Yokogawa Europe BV, Amersfoort, The Netherlands) prior to the experiment. The data were fitted using the two-site competition equation of Origin 6.0, leading to estimation of the two pK_a values.

Chemical Modification of Histidine Residues of AsLOV2 Using Diethyl Pyrocarbonate (DEPC). AsLOV2 in 20 mM Tris-HCl and 50 mM NaCl (pH 8) was incubated at room temperature with 5 mM DEPC from a 6 M stock solution. This latter chemical is a histidine-specific reagent which can inactivate histidine function and thereby abolished its base catalysis properties. DEPC can also react with tyrosine residues; however, upon addition of DEPC, no change at 280 nm could be detected in the UV−vis spectrum of the protein (data not shown). We can therefore exclude tyrosine modification under our experimental conditions. Transient slow UV−vis measurements were performed before and after incubation for 15 min with DEPC.

RESULTS AND DISCUSSION

Imidazole Reversibly Enhances the Dark Recovery Rate of AsLOV2. In this investigation, we found that the AsLOV2 dark state recovery rate was markedly enhanced by exogenously added imidazole. Figure 2 shows the dark state recovery of AsLOV2 at different imidazole concentrations ranging from 0 to 50 mM. The dark recovery time constant of AsLOV2 was ~30 s in the absence of imidazole at pH 8, which agrees well with previously reported values (*8*, *15*). Complete recovery of the dark state is observed in ~10 and ~1 s for 2 and 50 mM imidazole, respectively. The level of bleaching at 475 nm under constant illumination decreases with an increase in imidazole concentration from 0.45 to 0.06 for 0 and 50 mM imidazole, consistent with the increased thermal recovery reaction rate induced by imidazole. Indeed, the steady state equilibrium under continuous illumination in the presence of 50 mM imidazole is dependent on light intensity (data not shown). No change in the UV−vis absorption spectrum of either D_{447} or S_{390} is observed for imidazole concentrations up to 1 M at room temperature.

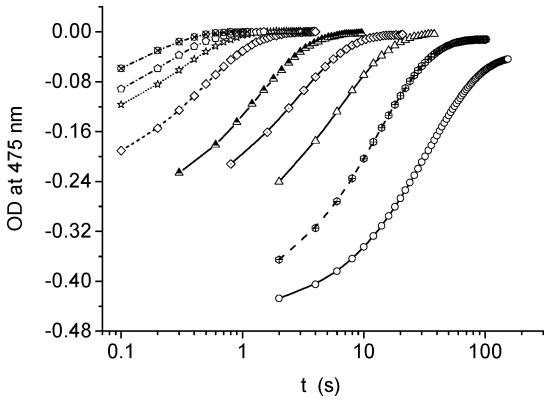

FIGURE 2: Dark state recovery of AsLOV2 at different imidazole concentrations, in decreasing time constant order: 0, 0.4, 1, 2, 4, 10, 20, 30, and 50 mM. Kinetics were measured at room temperature between 280 and 550 nm with a model 8453 Hewlett-Packard diode array spectrophotometer (time resolution of 0.1 s). Here only the 475 nm time trace is shown.

A more complete kinetic investigation of the imidazole effect has been performed in the range from 0 to 100 mM and from 150 to 660 mM by combining slow and fast time-resolved measurements, respectively. Using ~40 μM AsLOV2 (ϵ = 13 800 M^{-1} cm^{-1}) in 20 mM Tris-HCl and 50 mM NaCl (pH 8), adduct cleavage was enhanced ~2-, ~10-, ~100-, and ~4000-fold with addition of 0.5, 2, 20, and 660 mM imidazole, respectively (Figure 3). The recovery rate is linearly dependent on imidazole concentration in the range from 0 to 660 mM, indicating a first-order kinetic effect. For all imidazole concentrations, AsLOV2 adduct decay could be fitted adequately with a single exponential, and the resulting time constant shows a linear dependence on imidazole concentration. Thus, no additional spectroscopically distinguishable intermediates are formed by imidazole in the dark recovery reaction. Upon dilution of a sample containing 100 mM imidazole, using overnight dialyses, the dark recovery time constant in the absence of imidazole (30 s) is recovered, indicating that the effect of imidazole is fully reversible.

The addition of imidazole to several other LOV domains shows a similar enhancement of the thermal decay rate: from $(240\ s)^{-1}$ to $(1\ s)^{-1}$ at 20 mM imidazole in *Adiantum* phy3 LOV2 (phy3LOV2). In CrLOV2, which shows a biphasic dark recovery (*19*), the fast component (from 30 to 0.18 s with 100 mM) is 4 times more sensitive to imidazole (expressed as fold enhancement) than the slow one (from

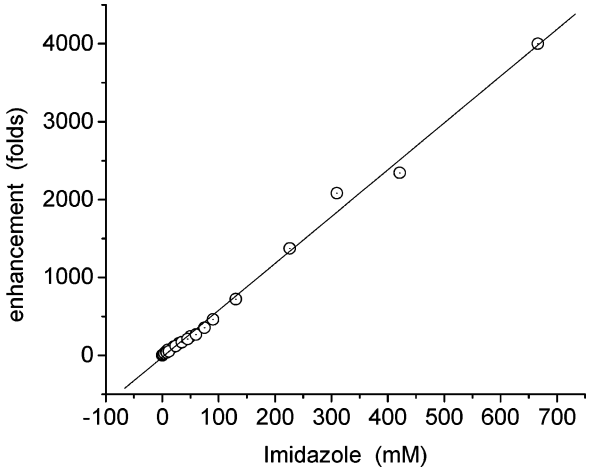

FIGURE 3: Enhancement of the thermal back reaction rate of AsLOV2 (in fold stimulation) plotted vs imidazole concentration. The plot combines slow and fast time-resolved measurements of the recovery rate of AsLOV2 as a function of imidazole concentration.

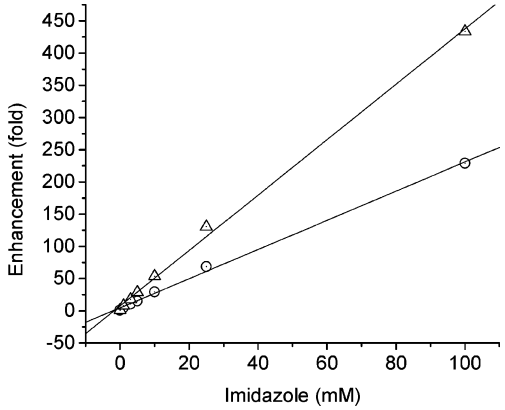

FIGURE 4: Enhancement of the recovery rate of AsLOV2 as a function of imidazole concentration at pH 8 (△) and 7 (○). The ratio of the fold enhancement between the two data sets varies between 1.7- and 1.9-fold, which is expected considering that at pH 7 and 8, 53 and 92% of the imidazole is present in the basic form, respectively.

115 to 2.5 s with 100 mM). This result may be correlated with the different activation energy barriers for the biphasic adduct cleavage that have been determined for CrLOV2, of 52 and 72 kJ/mol for the fast and slow component, respectively (*19*). We cannot exclude, however, that the different sensitivities could be due to differences in accessibility for imidazole toward two structurally distinct populations (e.g., as the result of a CrLOV2 monomer−dimer equilibrium).

We tested whether the imidazole effect was dependent on protein concentration: at 0.1 mM imidazole, the recovery rate is dependent on protein concentration in the range from 0.03 to ~1 mM (equivalent to an OD of 0.35−12 at 447 nm) with recovery time constants ranging from 32 to 24 s (Figure S1 of the Supporting Information). We conclude that imidazole forms a very low-affinity Michaelis−Menten complex with AsLOV2, without significantly disturbing the electronic state of FMN. This complex has a very high K_d (corresponding to a low affinity) with k_{on} and k_{off} rates that are very fast, much faster than the rate of adduct decay. A linear dependence of the thermal decay rate as a function of imidazole concentration has already been reported for the blue light photoreceptor AppA (*25*) and in rescue experiments using imidazole as an exogenous ligand for luciferase (*26*), horseradish peroxidase (*26*, *27*), and ribozyme (*27*). In all these studies, the K_d was estimated to be larger than several molar. However, in these rescue experiments, the activity is restored with millimolar concentrations of imidazole, showing that under such conditions imidazole and protein or catalytic RNA (ribozyme) form a discrete complex prior to catalysis.

pH Dependence of the Imidazole Effect. To determine which form of imidazole, i.e., the acidic or basic form, is responsible for the observed effects, we conducted kinetic assays at different imidazole concentrations (ranging from 0 to 100 mM) at pH 7 and 8. The concentration and pH dependence of the pseudo-first-order recovery rate constant for AsLOV2 in imidazole at pH 7 and 8 are shown in Figure 4. The pK_a of imidazole is 6.95; thus at pH 7 and 8, 53 and 92% of the imidazole resides in the basic form, respectively. For the different imidazole concentrations that were used, the enhancement of the dark recovery rate is between 1.7 and 1.9 times less efficient at pH 7 than at pH 8. This result agrees well with the ratio of 1.74 calculated for the abundance of the basic and acidic form of imidazole under these conditions, respectively. Thus, the basic form of imidazole is likely responsible for the enhancement of the rate of the dark recovery. These data are consistent with an imidazole-enhanced dark recovery by a general base-catalyzed mechanism.

Specific, Discrete Effect of an Imidazole Base. To obtain additional insights into the base-catalyzed mechanism mediated by imidazole, we tested the effect of imidazole analogues (Figure 1b). Interestingly, histidine did not have any effect (up to concentrations of 100 mM), indicating that the imidazole base does not act from the LOV domain surface. Thus, it could be either its size (153 Å^3 for histidine vs 65 Å^3 for imidazole) or its polarity (both amines and carboxylates are charged at pH 8) which precludes the action of histidine. We thus investigated the effectiveness of imidazole analogues with similar sizes but different polarities. 1-Methylimidazole (molecular structure shown in Figure 1b) is more hydrophobic than imidazole with a very similar pK_a (7.1) and exhibits a slightly higher efficiency (1.3 times) in enhancing the rate of dark recovery of AsLOV2 at pH 8 as compared to imidazole, when tested at equimolar concentrations. Specifically, at 20 and 80 mM 1-methylimidazole, 130- and 450-fold enhancement of the recovery rate of AsLOV2 is observed, respectively, compared to 100- and 350-fold for imidazole, respectively. An even more hydrophobic analogue, dimethylaminopyridine (DMAP, molecular structure shown in Figure 1b), with a pK_a of 9.7, shows a significant effect at pH 8 where less than 2% of the DMAP molecules are in the basic form, indicating that this molecule is a very efficient enhancer of the dark recovery rate of AsLOV2. Indeed, the latter molecule exhibited an only 2-fold lower efficiency as compared to that of imidazole at pH 8 in the range from 0 to 10 mM DMAP. To properly compare both molecules, the effect of DMAP was studied at pH 10, where more than 50% of the molecules reside in the basic form. At pH 10, DMAP is slightly more efficient than imidazole. Because at this pH imidazole resides entirely in its basic form, compared to ~55% for DMAP, DMAP is approximately 2 times more efficient than imidazole in performing the catalysis. This

increased efficiency of DMAP is very likely due to its increased hydrophobicity. Moreover, the acceleration by DMAP shows that the pK_a of the AsLOV2 reactive cysteine is higher than 9.7 which is rather high for an aqueous thiol.

Azide (HN_3), a small molecule with a pK_a of 4.8, had no obvious effect on the thermal decay of S_{390} of AsLOV2 at pH 8 up to concentrations of 100 mM. Azide has been reported in bacteriorhodopsin to shuttle protons from the solvent to the protein interior, increasing the decay rate of the M intermediate (i.e., Schiff base reprotonation) (*28*). The lack of an effect of azide can be due to its negative charge at pH 8 which could disfavor its binding to AsLOV2 and/or its low pK_a.

The question of whether the base-mediated catalysis destabilizes the light state of the protein via a protein-assisted recovery or acts directly on the cysteinyl−N5 covalent adduct arises. Dark recovery enhanced by imidazole has already been shown in AppA, albeit with a 100-fold lower efficiency (*25*). There, the authors concluded that imidazole was acting on the protein surface rather than on the H-bond network directly responsible for the stability of the light-induced signaling state. To test if the imidazole effect is due to disruption of noncovalent interactions leading to destabilization of the secondary and tertiary structure and/or disorganization of the H-bond network in the vicinity of the FMN moiety of the LOV2 domain in a nonspecific way, the effect of guanidinium chloride (GnCl, chaotropic salt) on the rate of dark recovery was measured at various concentrations of this denaturant. We found that GnCl has a very weak effect up to 500 mM, and when half of the LOV2 domains are unfolded at 3 M GnCl, an only 3-fold increase of the recovery rate is observed (data not shown). These results exclude the interpretation that imidazole acts in a nonspecific way by destabilizing the PAS fold of AsLOV2. As its influence is very weak and incompatible with the 3 order of magnitude change induced by imidazole, this suggests a direct interaction of imidazole molecules with the adduct state and the acceleration of the limiting step of the reaction via a base-catalyzed mechanism.

Imidazole Acts in the Vicinity of FMN. No significant change was observed in the absorption spectrum of AsLOV2 between 400 and 500 nm at room temperature in the presence of imidazole up to 1 M at room temperature. The dark recovery rate varied linearly with the imidazole concentration, without any saturation effect up to 660 mM, which precludes an estimate of the K_d of imidazole binding. However, at 77 K, a 0.5 and 1.5 nm red shift of the absorption spectrum, with isosbestic points at 428, 448, 464, 471, and 478 nm, is observed in the presence of 0.2 and 0.5 M imidazole, respectively. This observation suggests the formation of a AsLOV2−imidazole complex upon addition of imidazole (Figure 5). The red shift probably results from a weak H-bond between imidazole and the FMN N(5) atom or to one of its C═O groups, leading to a more delocalized FMN-conjugated system. Such small absorption changes have been observed in rescue experiments of a His to Ala mutant of horseradish peroxidase, in which imidazole binds to the cavity created by the mutation, restoring enzyme activity and coordination of the heme to the iron atom. In similar experiments for choline oxidase (*29*) and luciferase (*26*), two flavin-binding enzymes, no spectral changes were detected upon imidazole addition, suggesting that the visible absorption of the flavin is relatively insensitive to a nearby bound imidazole molecule.

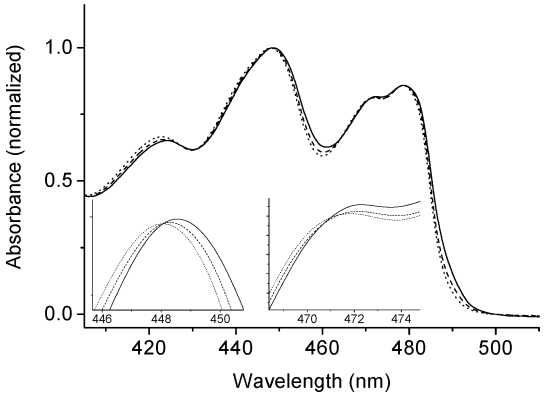

FIGURE 5: Low-temperature (77 K) absorption spectra of AsLOV2 at different imidazole concentrations: no imidazole (···), 200 mM imidazole (- - -), and 500 mM imidazole (—). Insets are zooms on two isosbestic points at 448 (left) and 471 nm (right).

Cavity Identification in the Crystal Structure of the Phy3LOV2 Domain. The fact that histidine has no effect on the dark recovery rate of AsLOV2, as opposed to neutral basic imidazole and its hydrophobic analogues, with an increased efficiency for the latter, suggests that the base-catalyzed activity takes place from a hydrophobic locus within the PAS fold. Histidine, which has the same base catalysis properties as imidazole, is able to explore the surface of AsLOV2 but has no effect, suggesting that base catalysis does not take place from the AsLOV2 surface. In such a context, two interpretations appear to be likely.

First, imidazole and its hydrophobic analogues may be dissolved nonspecifically in the hydrophobic core of AsLOV2 and interact specifically with the FMN−cysteinyl adduct. The dynamic motions of the protein would allow the hydrophobic molecules to enter and reside in the core. However, such solubilization of a hydrophobic molecule within the PAS fold would affect specific interactions and would be expected to lead to unfolding of the PAS domain at high concentrations, which is not observed experimentally.

Second, a specific tunnel cavity structure may exist that allows specific entry and binding of imidazole and its hydrophobic analogues but restricts histidine from entering it by size and/or charge exclusion. Such an interpretation is consistent with the work of Rudiger and Briggs, who have indicated a role for a hydrophobic cavity in light-activated autophosphorylation of phototropin in plasma membranes isolated from the tips of maize coleoptiles by use of several thiol reagents (*33*). Considering the small size of the LOV domain, this cavity is likely to be close to the FMN binding site.

To test this hypothesis, we used three software packages [Deep View (spdbv), UCSF Chimera, and PyMol (Caver)] to compute cavities and channels in the four different molecules of the unit cell of the structures of the dark and light states of phy3LOV2 (PDB entries 1G28 and 1JNU, respectively). All calculations show the presence of two main hydrophobic cavities located 4−5 Å from the isoalloxazine moiety. The first one is located above the dimethylbenzene plane and has a volume of ∼30−40 Å^3 (Deep View). The second cavity is larger, with a volume of ∼40−60 Å^3 and is located between the C(4)═O group and the PAS fold surface.

We emphasize that the computed cavities should not be regarded as static voids in the PAS core: since the crystal structures represent average structures and the protein is highly dynamic, the cavities indicate the sites where on average more space is available for small molecule binding than elsewhere in the hydrophobic core.

The volume of the cavities is slightly larger in the light state than in the dark state which suggests that the imidazole binding site is more accessible in the light state. Considering the imidazole volume of 65 Å^3, we expect the larger cavity to be a good candidate for imidazole binding. Moreover, light-induced protein structural changes have been found to be relatively small in crystals, whereas in solution, NMR spectroscopy (*24*) and FTIR light minus dark spectra of AsLOV2 (*16*) and phy3LOV2 (*22*, *34*) show significant protein structural changes. Interestingly, PYP exhibits the same difference in behavior in solution compared to the crystalline state (*35*). Thus, a larger imidazole accessibility of the LOV2 light state may be expected under our experimental conditions (solution) compared to the crystalline state.

The first phy3LOV2 cavity is surrounded by the dimethylbenzene moiety of the isoalloxazine ring of FMN and protein residues I943, N965, T934, and V932; the second cavity is surrounded by the FMN C(4)═O group and residues F950, F1006, L969, L953, T954, and N1008. Both cavities are quite hydrophobic, which could explain the slightly higher efficiency of 1-methylimidazole and the even higher efficiency of DMAP. It also explains the exclusion of imidazolium (the acidic form of imidazole), histidine, and azide and the very fast k_{on}/k_{off} rates of the imidazole base.

A more thorough molecular surface study, using Chimera, shows the structure of the second cavity, which exhibits two narrow channels that point toward the LOV surface. The longest channel reaches the surface by forming a "hole". The latter is located between the αA helix and the bottom of the five β-strands, forming a "cliff", further identified as a potential imidazole binding site on the PAS fold surface by Chimera. Strikingly, similar cavity−channel−surface structures are observed in the crystal structure of CrLOV1 (*10*), PYP (*36*), and NifL (*37*), suggesting that it is an intrinsic structural property of the PAS fold. Nevertheless, imidazole did not have any observable effect on the photocycle kinetics of PYP (data not shown). Because the first, smaller, cavity does not show any opening to the solvent, the highest population of imidazole molecules is to be expected in the cavity located between the surface and the FMN C(4)═O group. To test this hypothesis, we used the Caver plug-in in PyMol to specifically compute channels. As expected, the first cavity is connected to the surface via very narrow channels while the second cavity shows three channels, starting 3−4 Å from the FMN/C(4)═O group and pointing toward the same (Chimera) hole in the surface, following slightly different routes. For the purpose of clarity, only one of these channels is shown in Figure 6. This observation is consistent with the red shift of the low-temperature absorption spectrum, which suggests a weak H-bond interaction between imidazole and the FMN N(5) or C═O group.

Mechanism of the Imidazole Base-Catalyzed Accelerated Dark Recovery of AsLOV2. By fitting an imidazole molecule in the computed cavity using DeepView and/or Chimera, we can show that its two nitrogen atoms are located ~4−5 Å

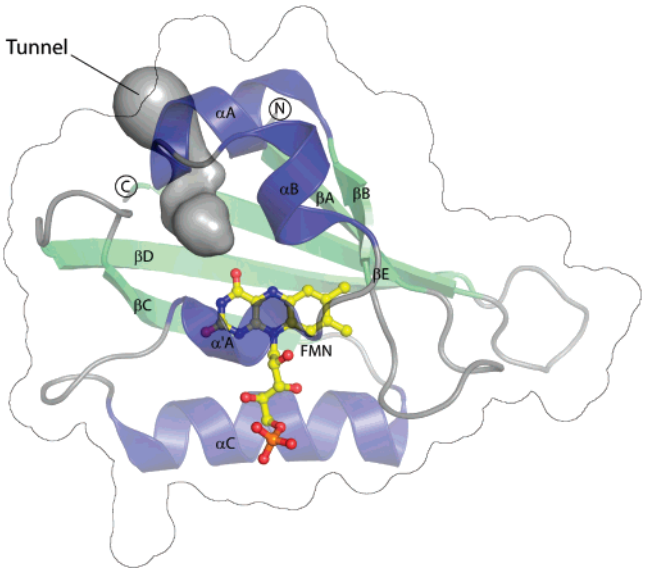

FIGURE 6: PyMol-Caver picture showing the structure of one of the channels (tunnel), joining the large cavity located 3−5 Å from the FMN C(4)═O moiety with the protein surface of the LOV2Phy3 dark state (PDB entry 1G28). The channel pointing toward the surface is colored gray and FMN yellow. α-Helices are colored blue; the β-sheet is colored green, and the surface is shown as an outline.

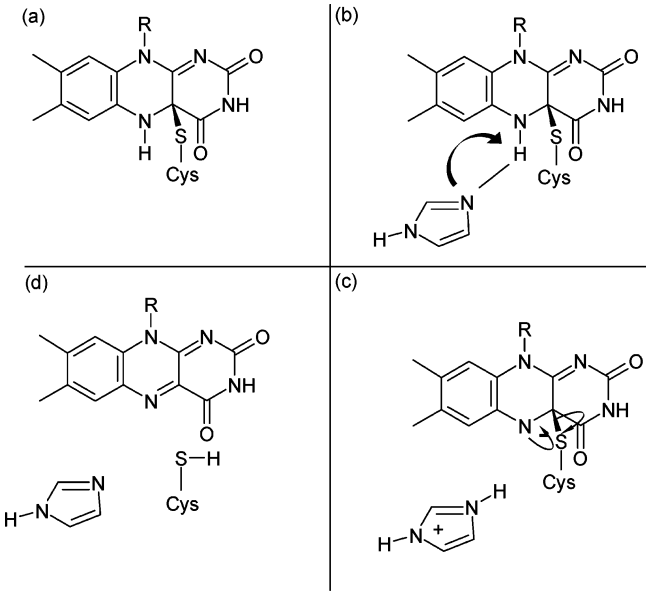

FIGURE 7: Proposed ionic base-catalyzed mechanism to account for the imidazole-mediated acceleration of the dark state recovery of *A. sativa* phot1 LOV2. See the text for further details.

from the FMN N(5) atom, which carries a hydrogen in the light state. Such proximity could explain the surprisingly high imidazole sensitivity (a more than 4000-fold increase in the recovery rate at 0.66 M) of AsLOV2, pointing toward a mechanism in which the FMN N(5) proton is directly abstracted in an imidazole-induced base-catalyzed mechanism. Thus, we propose that the imidazole base accesses the vicinity of the FMN binding site, with particularly high efficiency in the light state (Figure 7b), via the channels leading to the C(4)═O cavity. Imidazole within this cavity does not disturb FMN binding, as FMN is neither released nor significantly altered with respect to its spectral properties of the light and dark state UV−vis absorption spectra up to 1 M imidazole at room temperature. Imidazole is in fast

equilibrium between the inside and outside of this cavity, which explains the linear imidazole concentration dependence. If specific binding occurs in this cavity, its K_d should be on the order of several molar. Because imidazole acts on FMN from a few angstroms, the base-catalyzed reaction is assumed to be fast and efficient. In this context, a likely mechanism of base-catalyzed adduct rupture can be considered as outlined below.

Ionic Mechanism (concerted). The imidazole base presumably catalyzes the dark recovery by direct proton abstraction of the FMN N(5) atom (competing with the H-bonded Gln1029, phy3LOV2 numbering) which leads to the formation of a negatively charged adduct state intermediate, FMN C(4a)sp3(−)_S-Cys , and a positively charged imidazole (ImH_2^+, acidic form).

(i) First, the lone pair of the N atom of imidazole will attack the proton of the N(5) atom and bind it (Figure 7b). The mechanism can also be concerted, leading to an imidazole hydrogen-bonded to the FMN N(5)−H bond creating an electropositive ImH-H base and an electronegative Cys-S-C(4a)-N(5) conjugated network where the sulfur attracts the electrons as proposed by Swartz et al. (*8*).

(ii) Second, the electrons of the N(5)−H bond will then form a double bond between N(5) and C(4a), which (iii) in turn will lead to disruption of the C(4)−S bond and formation of the thiolate anion (Figure 7c). These events likely induce a reversible switch of the Gln, which H-bonds back to the FMN C(4)═O group. (iv) The last step then is protonation of the Cys anion by the protonated imidazole, regenerating both the noncovalently bound oxidized FMN and the imidazole base (Figure 7d).

The effect of imidazole on AsLOV2 confirms that the proton transfer step is the rate-limiting step of the dark recovery reaction (*8*, *38*). Thus, by accelerating the rate-limiting step of the recovery reaction, the presence of the imidazole base leads to such a drastic increase in its rate of dark recovery.

pH Titration of the Adduct Decay Rate of AsLOV2. With regard to the high efficiency of the imdazole base-catalyzed dark recovery of the AsLOV2 domain, the question of whether histidine residues in the native structure can act as base catalysts of the dark recovery reaction arises. To investigate the involvement of histidine residues in the thermal recovery of AsLOV2, we performed a pH titration of the dark recovery time constant (Figure 8). The pH titration was already reported by Corchnoy et al. and was found to exhibit a pK_a of 6.8 (*38*). We repeated these experiments to verify our experimental conditions. The titration curve between pH 6.4 and 11.5 was best fitted using two pK_a values, with a first pK_a of 7.2 with an associated amplitude of 0.8 and a second pK_a of 11.2 with an amplitude of 0.2. The first pK_a of 7.2 compares well with the value of 6.8 reported by Corchnoy et al. (*38*) and can be assigned to a histidine residue or the FMN phosphate group, although it is quite high compared to the pK_a of phosphate of 6.2 in solution. The second pK_a was not resolved in the previous study, where the titration stopped below pH 10. It represents a crude estimate, considering the fact that the pH range above 11.5 was not accessible because of the limited stability of the protein. The second pK_a may tentatively be assigned to deprotonation of the N(3) atom of FMN, which has a pK_a of 9.75 in solution (*39*) which shifts to ∼11 in AsLOV2

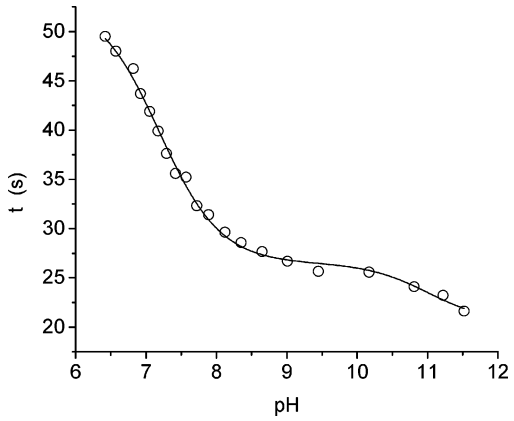

FIGURE 8: pH titration of the dark recovery time constant of AsLOV2 in the pH range of 6.4−11.5. The data have been fitted using a double-pK_a Henderson−Hasselbalch equation (black line).

(*8*). The dark recovery time constant increases by a factor of 2, going from 50 s at pH 6.4 to 25 s at pH 9.5, comparing well with previously reported data (*38*).

Histidine as an Intrinsic Base Catalyst in AsLOV2: Chemical Modification of Histidine Residues by Diethyl Pyrocarbonate (DEPC). One can wonder whether the positioning of histidine residues within the PAS fold and the stabilization of their protonated state, e.g., acidic (inactive) or basic (active), can tune the dark recovery rate. To address this question, we performed a measurement of the dark recovery rate as a function of pH and we chemically modified the two conserved (among the phot1/2 LOV2 family) surface-exposed histidine residues of AsLOV2 (His1011 and -1035, phy3LOV2 numbering) by incubating them with an excess of the histidine-specific reagent DEPC (*40*). At pH 8, the recovery time constant is 30 s in the absence of DEPC and 65 s in the presence of 5 mM DEPC, demonstrating a significant effect that may be attributed to histidine modification (Figure S2 of the Supporting Information). We can now make a quantitative relation among the total thermal recovery rate (k_{th}) in the absence of DEPC, the rate of adduct rupture mediated by processes other than base catalysis (k_{other}) after DEPC inactivation, and the histidine-mediated base catalysis rate (k_{HBC}) via the relation

$$k_{th} = k_{HBC} + k_{other}$$

This experiment indicates that the rate of histidine-mediated base catalysis (k_{HBC}) at pH 8 amounts to $(30\ s)^{-1} - (65\ s)^{-1} = (55\ s)^{-1}$, where ∼92% of histidine molecules are in the basic active form. A good correlation is found between the pH titration and the histidine inactivation experiment in the sense that plotting the fraction of histidines in the basic form as a function of the decay time constant gives a linear function which extrapolates to 62 s for 0% of the basic form (data not shown). The predicted time constant of 62 s for 0% of the basic form of histidine is close to 65 s when all histidines are inactivated by DEPC and indicates that a molecular process other than histidine-mediated base catalysis contributes significantly to the total thermal decay rate of the adduct in AsLOV2 by a rate constant k_{other} of $(65\ s)^{-1}$. In addition, the linear behavior of that latter plot confirms that only one pK_a is observable around 7, leading to the conclusion that only one of the two histidines is active or that the two have approximately the same pK_a. This experi-

ment allows us to estimate the contribution of histidine residues in the catalysis of thermal adduct decay, showing that as in the case of exogenously added imidazole, the basic form of histidine constitutes the base catalyst in this reaction.

Thus, as proposed by Swartz et al. (*8*), at least in AsLOV2, base catalysis can take place from surface-exposed histidine residues to the FMN, localized 12 Å away, via a postulated hydrogen bonding network of the base, chromophore, and intraprotein water molecules. The relatively low efficiency (factor of 2 only) of the histidine base-catalyzed mechanism in AsLOV2 can be explained in terms of distance, as suggested by the imidazole effect which increases the decay rate by at least 3 orders of magnitude when it is used as an exogenous ligand acting in the FMN vicinity.

CONCLUSIONS

Imidazole greatly enhances the thermal decay rate of the covalent adduct in several LOV domains, such as *A. sativa* phot1 LOV2, *Adiantum* phy3LOV2, and *Chlamydomonas* phot LOV2, extending its action on LOV domains from plants to green algae. The general base catalysis mechanism for imidazole, or an imidazole side chain, as proposed for the process studied here is supported by a strong precedent for exogenous imidazole acting as a general base catalyst, for example, in AppA and in the rescue of the activity of histidine mutations of bacterial luciferase (H44A) and horseradish peroxidase (H42A). Furthermore, evidence of the role of imidazole, or an imidazole side chain, as a general base in RNA cleavage reactions is available (*41*). The effect of imidazole on LOV and BLUF domain-containing photoreceptors shows that basic residues and especially histidines can be involved in the tuning of the thermal recovery rate of the adduct-containing signaling state. The extent of acceleration of the recovery rate using imidazole renders possible the application of time-resolved techniques which require relatively fast repetition rates, such as FTIR step-scan spectroscopy, which is at present under investigation in our laboratory.

ACKNOWLEDGMENT

We thank Jason Key for assistance in using PyMol-Caver software and in the design of Figure 6, Johnny Hendriks for assistance with the flash-photolysis measurements, and Marcela Avila-Perez and Jason Key for thoughtful discussions. The *A. sativa* LOV2 construct was kindly provided by Kevin Gardner from the Univeristy of Texas Southwestern Medical Center. The MBP−CrLOV2 sample was kindly donated by Peter Hegemann (Humboldt University). Cavity volume computations were estimated using Swiss-pdb-Viewer (Deep-View). Molecular graphics computations were produced using the UCSF Chimera package from the Resource for Biocomputing, Visualization, and Informatics at the University of California (San Francisco, CA) (supported by NIH Grant P41 RR-01081). Channels computation was performed using PyMol-Caver (DeLano Scientific, San Carlos, CA).

SUPPORTING INFORMATION AVAILABLE

Dark state recovery time constant of AsLOV2 plotted as a function of protein concentration in presence of 100 mM imidazole (Figure S1). At pH 8, the recovery time constant of AsLOV2 is 30 s in the absence of DEPC and 65 s in the presence of 5 mM DEPC, demonstrating a significant effect that may be attributed to histidine modification (Figure S2). This material is available free of charge via the Internet at http://pubs.acs.org.

REFERENCES

1. Christie, J. M., and Briggs, W. R. (2005) in *Handbook of Photosensory Receptors* (Briggs, W. R., and Spudich, J. L., Eds.) pp 277−304, Wiley-VCH Verlag GmbH & Co., Weinheim, Germany.
2. Christie, J. M., Reymond, P., Powell, G. K., Bernasconi, P., Raibekas, A. A., Liscum, E., and Briggs, W. R. (1998) *Arabidopsis* NPH1: A flavoprotein with the properties of a photoreceptor for phototropism, *Science 282*, 1698−1701.
3. Losi, A. (2004) The bacterial counterparts of plant phototropins, *Photochem. Photobiol. Sci. 3*, 566−574.
4. Crosson, S., Rajagopal, S., and Moffat, K. (2003) The LOV domain family: Photoresponsive signaling modules coupled to diverse output domains, *Biochemistry 42*, 2−10.
5. Ballario, P., Talora, C., Galli, D., Linden, H., and Macino, G. (1998) Roles in dimerization and blue light photoresponse of the PAS and LOV domains of *Neurospora crassa* white collar proteins, *Mol. Microbiol. 29*, 719−729.
6. Imaizumi, T., Tran, H. G., Swartz, T. E., Briggs, W. R., and Kay, S. A. (2003) FKF1 is essential for photoperiodic-specific light signalling in *Arabidopsis*, *Nature 426*, 302−306.
7. He, Q. Y., Cheng, P., Yang, Y. H., Wang, L. X., Gardner, K. H., and Liu, Y. (2002) White collar-1, a DNA binding transcription factor and a light sensor, *Science 297*, 840−843.
8. Swartz, T. E., Corchnoy, S. B., Christie, J. M., Lewis, J. W., Szundi, I., Briggs, W. R., and Bogomolni, R. A. (2001) The photocycle of a flavin-binding domain of the blue light photoreceptor phototropin, *J. Biol. Chem. 276*, 36493−36500.
9. Crosson, S., and Moffat, K. (2001) Structure of a flavin-binding plant photoreceptor domain: Insights into light-mediated signal transduction, *Proc. Natl. Acad. Sci. U.S.A. 98*, 2995−3000.
10. Fedorov, R., Schlichting, I., Hartmann, E., Domratcheva, T., Fuhrmann, M., and Hegemann, P. (2003) Crystal structures and molecular mechanism of a light-induced signaling switch: The Phot-LOV1 domain from *Chlamydomonas reinhardtii*, *Biophys. J. 84*, 2474−2482.
11. Kennis, J. T. M., Crosson, S., Gauden, M., van Stokkum, I. H. M., Moffat, K., and van Grondelle, R. (2003) Primary reactions of the LOV2 domain of phototropin, a plant blue-light photoreceptor, *Biochemistry 42*, 3385−3392.
12. Kottke, T., Heberle, J., Hehn, D., Dick, B., and Hegemann, P. (2003) Phot-LOV1: Photocycle of a blue-light receptor domain from the green alga *Chlamydomonas reinhardtii*, *Biophys. J. 84*, 1192−1201.
13. Crosson, S., and Moffat, K. (2002) Photoexcited structure of a plant photoreceptor domain reveals a light-driven molecular switch, *Plant Cell 14*, 1067−1075.
14. Salomon, M., Eisenreich, W., Durr, H., Schleicher, E., Knieb, E., Massey, V., Rudiger, W., Muller, F., Bacher, A., and Richter, G. (2001) An optomechanical transducer in the blue light receptor phototropin from *Avena sativa*, *Proc. Natl. Acad. Sci. U.S.A. 98*, 12357−12361.
15. Salomon, M., Christie, J. M., Knieb, E., Lempert, U., and Briggs, W. R. (2000) Photochemical and mutational analysis of the FMN-binding domains of the plant blue light receptor, phototropin, *Biochemistry 39*, 9401−9410.
16. Swartz, T. E., Wenzel, P. J., Corchnoy, S. B., Briggs, W. R., and Bogomolni, R. A. (2002) Vibration spectroscopy reveals light-induced chromophore and protein structural changes in the LOV2 domain of the plant blue-light receptor phototropin 1, *Biochemistry 41*, 7183−7189.
17. Kasahara, M., Swartz, T. E., Olney, M. A., Onodera, A., Mochizuki, N., Fukuzawa, H., Asamizu, E., Tabata, S., Kanegae, H., Takano, M., Christie, J. M., Nagatani, A., and Briggs, W. R. (2002) Photochemical properties of the flavin mononucleotide-binding domains of the phototropins from *Arabidopsis*, rice, and *Chlamydomonas reinhardtii*, *Plant Physiol. 129*, 762−773.
18. Kennis, J. T. M., van Stokkum, I. H. M., Crosson, S., Gauden, M., Moffat, K., and van Grondelle, R. (2004) The LOV2 domain

of phototropin: A reversible photochromic switch, *J. Am. Chem. Soc. 126*, 4512−4513.
19. Guo, H. M., Kottke, T., Hegemann, P., and Dick, B. (2005) The Phot LOV2 domain and its interaction with LOV1, *Biophys. J. 89*, 402−412.
20. Losi, A., Polverini, E., Quest, B., and Gartner, W. (2002) First evidence for phototropin-related blue-light receptors in prokaryotes, *Biophys. J. 82*, 2627−2634.
21. Losi, A., Kottke, T., and Hegemann, P. (2004) Recording of blue light-induced energy and volume changes within the wild-type and mutated Phot-LOV1 domain from *Chlamydomonas reinhardtii*, *Biophys. J. 86*, 1051−1060.
22. Iwata, T., Nozaki, D., Tokutomi, S., and Kandori, H. (2005) Comparative investigation of the LOV1 and LOV2 domains in *Adiantum* phytochrome3, *Biochemistry 44*, 7427−7434.
23. Nozaki, D., Iwata, T., Ishikawa, T., Todo, T., Tokutomi, S., and Kandori, H. (2004) Role of Gln1029 in the photoactivation processes of the LOV2 domain in *Adiantum* phytochrome3, *Biochemistry 43*, 8373−8379.
24. Harper, S. M., Neil, L. C., and Gardner, K. H. (2003) Structural basis of a phototropin light switch, *Science 301*, 1541−1544.
25. Laan, W., Gauden, M., Yeremenko, S., van Grondelle, R., Kennis, J. T. M., and Hellingwerf, K. J. (2006) On the mechanism of activation of the BLUF domain of AppA, *Biochemistry 45*, 51−60.
26. Newmyer, S. L., Sun, J., Loehr, T. M., and deMontellano, P. R. O. (1996) Rescue of the horseradish peroxidase His-170 → Ala mutant activity by imidazole: Importance of proximal ligand tethering, *Biochemistry 35*, 12788−12795.
27. Newmyer, S. L., and deMontellano, P. R. O. (1996) Rescue of the catalytic activity of an H42A mutant of horseradish peroxidase by exogenous imidazoles, *J. Biol. Chem. 271*, 14891−14896.
28. Brown, L. S., and Lanyi, J. K. (1996) Determination of the transiently lowered pK_a of the retinal Schiff base during the photocycle of bacteriorhodopsin, *Proc. Natl. Acad. Sci. U.S.A. 93*, 1731−1734.
29. Ghanem, M., and Gadda, G. (2005) On the catalytic role of the conserved active site residue His(466) of choline oxidase, *Biochemistry 44*, 893−904.
30. Pettersen, E. F., Goddard, T. D., Huang, C. C., Couch, G. S., Greenblatt, D. M., Meng, E. C., and Ferrin, T. E. (2004) UCSF chimera: A visualization system for exploratory research and analysis, *J. Comput. Chem. 25*, 1605−1612.
31. DeLano, W. L. (2002) *PyMOL*, DeLano Scientific, San Carlos, CA.
32. Petrek, M., Otyepka, M., Banas, P., Kosinova, P., Koca, J., and Damborsky, J. (2006) CAVER: A new tool to explore routes from protein clefts, pockets and cavities, *BMC Bioinf. 7*, 316.
33. Rudiger, W., and Briggs, W. R. (1995) Involvement of Thiol-Groups in Blue-Light-Induced Phosphorylation of a Plasma Membrane-Associated Protein from Coleoptile Tips of Zea-Mays L, *Z. Naturforsch., C: J. Biosci. 50*, 231−234.
34. Iwata, T., Nozaki, D., Tokutomi, S., Kagawa, T., Wada, M., and Kandori, H. (2003) Light-induced structural changes in the LOV2 domain of *Adiantum* phytochrome3 studied by low-temperature FTIR and UV-visible spectroscopy, *Biochemistry 42*, 8183−8191.
35. Xie, A., Kelemen, L., Hendriks, J., White, B. J., Hellingwerf, K. J., and Hoff, W. D. (2001) Formation of a new buried charge drives a large-amplitude protein quake in photoreceptor activation, *Biochemistry 40*, 1510−1517.
36. Genick, U. K., Soltis, S. M., Kuhn, P., Canestrelli, I. L., and Getzoff, E. D. (1998) Structure at 0.85 Å resolution of an early protein photocycle intermediate [see comments], *Nature 392*, 206−209.
37. Key, J., Hefti, M., Purcell, E. B., Moffat, K. (2007) Structure of the redox sensor domain of *Azotobacter vinelandii* NifL at atomic resolution: Signaling, dimerization and mechanism, *Biochemistry*, in press.
38. Corchnoy, S. B., Swartz, T. E., Lewis, J. W., Szundi, I., Briggs, W. R., and Bogomolni, R. A. (2003) Intramolecular proton transfers and structural changes during the photocycle of the LOV2 domain of phototropin 1, *J. Biol. Chem. 278*, 724−731.
39. Drossler, P., Holzer, W., Penzkofer, A., and Hegemann, P. (2002) pH dependence of the absorption and emission behaviour of riboflavin in aqueous solution, *Chem. Phys. 282*, 429−439.
40. Godavarti, R., Cooney, C. L., Langer, R., and Sasisekharan, R. (1996) Heparinase I from *Flavobacterium heparinum*. Identification of a critical histidine residue essential for catalysis as probed by chemical modification and site-directed mutagenesis, *Biochemistry 35*, 6846−6852.
41. Perrotta, A. T., Shih, I. H., and Been, M. D. (1999) Imidazole rescue of a cytosine mutation in a self-cleaving ribozyme, *Science 286*, 123−126.

BI062074E